



# Comparison of choline influx from dynamic $^{18}\text{F}$ -Choline PET/CT and clinicopathological parameters in prostate cancer initial assessment

Xavier Palard-Novello<sup>1,2,3</sup> · Anne-Lise Blin<sup>1,3</sup> · David Bourhis<sup>4</sup> · Etienne Garin<sup>1,2,5</sup> · Pierre-Yves Salaün<sup>4,6,7</sup> · Anne Devillers<sup>2</sup> · Solène Querellou<sup>4,6,7</sup> · Patrick Bourguet<sup>1</sup> · Florence Le Jeune<sup>1,2,8</sup> · Hervé Saint-Jalmes<sup>1,2,3</sup>

Received: 29 January 2018 / Accepted: 26 February 2018 / Published online: 28 February 2018  
© The Japanese Society of Nuclear Medicine 2018

## Abstract

**Aim** The aim of the study was to compare the kinetic analysis of  $^{18}\text{F}$ -labeled choline (FCH) uptake with static analysis and clinicopathological parameters in patients with newly diagnosed prostate cancer (PC).

**Materials and methods** Sixty-one patients were included. PSA was performed few days before FCH PET/CT. Gleason scoring (GS) was collected from systematic sextant biopsies. FCH PET/CT consisted in a dual phase: early pelvic list-mode acquisition (from 0 to 10 min post-injection) and late whole-body acquisition (60 min post-injection). PC volume of interest was drawn using an adaptive thresholding (40% of the maximal uptake) on the late acquisition and projected onto an early static frame of 10 min and each of the 20 reconstructed frames of 30 s. Kinetic analysis was performed using an imaging-derived plasma input function. Early kinetic parameter (K1 as influx) and static parameters (early SUVmean, late SUVmean, and retention index) were extracted and compared to clinicopathological parameters.

**Results** K1 was significantly, but moderately correlated with early SUVmean ( $r=0.57$ ,  $p<0.001$ ) and late SUVmean ( $r=0.43$ ,  $p<0.001$ ). K1, early SUVmean, and late SUVmean were moderately correlated with PSA level (respectively,  $r=0.36$ ,  $p=0.004$ ;  $r=0.67$ ,  $p<0.001$ ;  $r=0.51$ ,  $p<0.001$ ). Concerning GS, K1 was higher for patients with  $\text{GS} \geq 4+3$  than for patients with  $\text{GS} < 4+3$  (median value  $0.409$  vs  $0.272 \text{ min}^{-1}$ ,  $p<0.001$ ). No significant difference was observed for static parameters.

**Conclusions** FCH influx index K1 seems to be related to GS and could be a non-invasive tool to gain further information concerning tumor aggressiveness.

**Keywords**  $^{18}\text{F}$ -Choline · Positron emission tomography · Prostate cancer · Kinetic analysis

## Introduction

Prostate cancer (PC) is the most commonly diagnosed cancer in male worldwide [1]. A number of studies have shown the usefulness of  $^{18}\text{F}$ -labeled choline (FCH) derivatives tracers for non-invasive positron emission tomography/computed tomography (PET/CT) in PC [2, 3]. Indeed, choline is a precursor of the biosynthesis of phosphatidylcholine, which is located on the cell membrane phospholipids and highly expressed in cancer, especially in PC [4–6]. To date, FCH PET/CT is mainly used for patients with recurrence of PC [7].

Concerning newly diagnosed PC, FCH PET/CT is mainly used to assess imaging abnormalities seen during intermediate-to-high-risk PC staging with pelvic magnetic resonance (MR), CT, and/or bone scan [8]. In general, for newly

✉ Xavier Palard-Novello  
x.palard@rennes.unicancer.fr

<sup>1</sup> University of Rennes 1, Rennes, France

<sup>2</sup> Department of Nuclear Medicine, Centre Eugène Marquis, Avenue de la Bataille Flandres-Dunkerque, 35000 Rennes, France

<sup>3</sup> UMR1099 INSERM, Rennes, France

<sup>4</sup> Department of Nuclear Medicine, Centre Hospitalier Universitaire, Brest, France

<sup>5</sup> UMR 1241 INSERM, Rennes, France

<sup>6</sup> University of Bretagne Occidentale, Brest, France

<sup>7</sup> EA 3878, Brest, France

<sup>8</sup> EA 4712, Rennes, France

diagnosed PC, staging and therapeutic options depends on the extent of the tumor (TNM), prostatic-specific antigen (PSA) level, Gleason Scoring (GS), number of biopsies involved with cancer, percentage of each biopsy involved with cancer, PSA doubling time, and life expectancy [9]. However, the utility of integrating novel prognostic factors into an updated risk stratification schema is still source of debate [10]. Indeed, overtreatment is a concern, because many of these cancers are not life-threatening. FCH PET/CT is a non-invasive procedure which could help in newly diagnosed PC to identify aggressive tumors, especially during active surveillance [11]. Therefore, FCH PET/CT could be added to the risk stratification schema in further studies.

Usually, the imaging protocol for FCH PET/CT consists in a dual-phase procedure: a pelvic kinetic acquisition starts immediately after tracer injection followed by a late scan covering the base of the skull through the superior portion of the thighs [12–14]. The early phase is mainly used to detect pelvic lesions before radioactive urine appears in the excretory pathways [12, 15, 16]. Moreover, this early acquisition could also be used to extract an FCH influx index using pharmacokinetic modeling [17–20]. Similar to the kinetic modeling of  $^{18}\text{F}$ -Fluorodeoxyglucose (FDG) PET/CT used for several cancers [19, 21–23], the kinetic modeling of FCH PET/CT in PC could add further information concerning tumor aggressiveness [24].

The aim of this study was to characterize the uptake of FCH using kinetic analysis in comparison with usual static parameters and GS in newly diagnosed PC.

## Materials and methods

### Patients

From October 2015 to April 2017, 61 patients with newly histologically proven PC and before any treatment referred to the nuclear medicine department to perform an FCH PET/CT were included. The study was approved by the institutional review board (2016.CE11). Before inclusion, each patient signed a written informed consent form after verbal and written explanations. All patients underwent  $^{18}\text{F}$  FCH PET/CT at least 14 days after US-guided biopsies to avoid any biopsy effect. Results of PSA test performed few days before FCH PET/CT were collected. GS were obtained from systematic extended-sextant 12-core biopsies, based on the Gleason System on ISUP criteria 2014 and stratified by categorization into low-grade ( $\text{GS} \leq 3 + 4$ ) and high-grade malignancies ( $\text{GS} > 3 + 4$ ), respectively.

### FCH PET/CT data

FCH was synthesized in Austria (IASOcholine; IASON GmbH, Austria). Each patient underwent a CT scan followed by a 10-min dynamic PET scan using list-mode acquisition with the field of view centered over the pelvic region. At the start of the PET acquisition, 3 MBq/kg were intravenously administered using an automated injector and flushed with 40 mL of saline. Two different PET/CT instruments were used: a Siemens Biograph mCT 64 camera and a Siemens Biograph mCT40 camera (Siemens, Knoxville, TN). Both systems have similar PET detector characteristics. All patients fasted at least 6 h before the FCH PET/CT scanning. A whole-body PET/CT scan was performed 1 h post-injection (p.i). PET data were reconstructed using point spread function based on time-of-flight 3D-ordered subsets expectation maximization iterative algorithm (2 iterations, 21 subsets) with corrections (attenuation, dead time, randoms, scatter, and decay) and 2 mm kernel convolution filter. Voxel size was  $4 \times 4 \times 2 \text{ mm}^3$ . Twenty frames of 30 s and 1 static frame of 10 min were reconstructed from the list-mode acquisition. Time-activity curve (TAC) from a volume of interest (VOI) was generated with the Syngo.via software (Siemens) by a nuclear medicine physician. The PC VOI was manually drawn on the late acquisition. Metabolic tumor volume was defined using an adaptive thresholding method based on the signal to noise ratio described by Daisne et al. [25]. The VOI was projected onto the early static frame of 10 min and each of the 20 reconstructed frames of 30 s. The standardized uptake value (SUV) was calculated and adjusted by means of an injected dose according to tissue activity concentration and patient body weight. The SUVmean of the metabolic tumor volume was measured on the early static frame of 10 min (early SUVmean) and on the late acquisition (late SUVmean). SUVmean parameter was preferred to SUVmax, because a lower number of counts is detected during the short duration of kinetic reconstructed frames. The retention index (%) was calculated as  $100 \times (\text{late SUVmean} - \text{early SUVmean}) / \text{early SUVmean}$ . For the kinetic analysis, an imaging-derived arterial input function was estimated from a manually-drawn VOI within the largest arterial blood-pool structures available on the early PET image when the peak blood-pool activity was the highest. For the tracer kinetic modeling, the reversible one-tissue compartment model with blood volume parameter was adopted, like recently published [17, 26]. Verwer et al. have suggested that this model is suitable for FCH kinetic modeling due to its robustness and consistency in shorter examinations [26]. Kinetic parameters were extracted with PMOD software version 3.8 (PMOD Technologies; Zürich, Switzerland).  $K_1$  ( $\text{min}^{-1}$ ) represented the influx between plasma compartment and tissue compartment.

## Statistical analysis

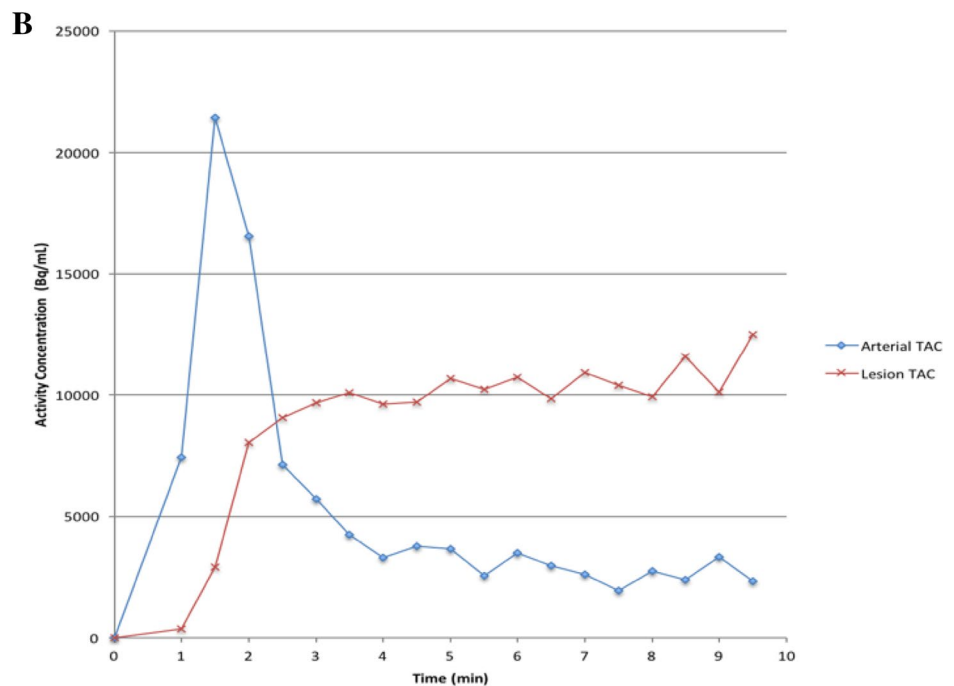
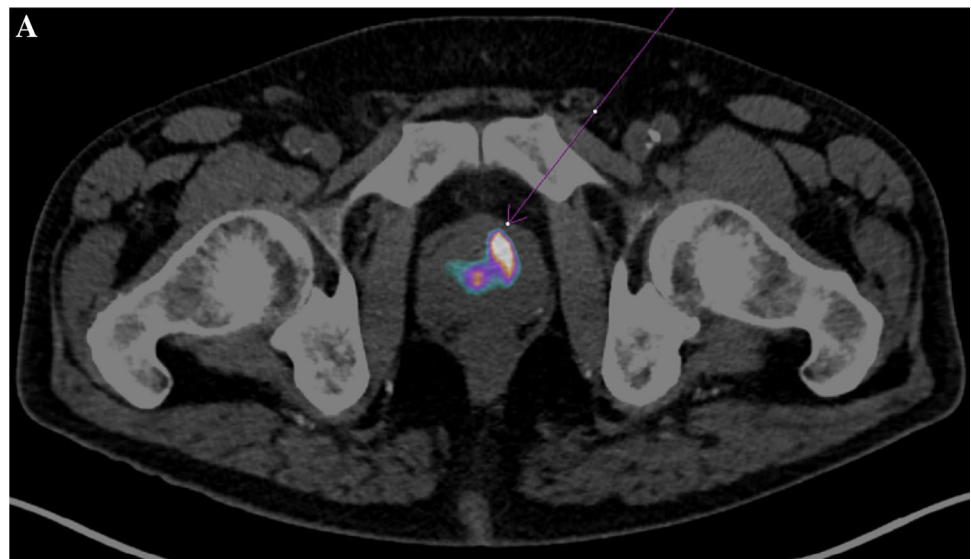
The Pearson's correlation test was performed to measure the statistical association between K1 and SUVs and between imaging parameters and PSA level. To compare imaging parameters and GS, a Mann–Whitney *U* test was performed. A *p* value < 0.05 was considered as statistically significant. A commercial program was used for all statistical analysis [Wolfram Research, Inc., Mathematica, Version 11.1, Champaign, IL (2017)].

## Results

### Patients

Median age was 65 years  $\pm$  7 (range 45–87). Thirty-nine patients showed tumor stage < T3 (8 as T1 and 31 as T2) and 22 patients showed tumor stage  $\geq$  T3 (21 as T3 and 1 as T4). At the time of FCH PET/CT, the median PSA level was 13.4  $\pm$  53.1 ng/mL (range 2.7–298). GS varied between 3 + 3 and 5 + 4 (15 as 3 + 3, 11 as 3 + 4, 15 as 4 + 3, 9 as 4 + 4, 9 as 4 + 5 and 2 as 5 + 4). Figure 1 shows TAC obtained in a 66 years old man.

**Fig. 1** A 66-year-old man with PSA level = 29 ng/mL. Fused axial early static frame FCH PET/CT (a) demonstrates prostatic uptake (purple arrow) with corresponding time-activity curves (b). FCH PET/CT parameters are:  $K_1 = 0.344 \text{ min}^{-1}$ ; early SUVmean = 2.2; late SUVmean = 3.4 and retention index = 55%. Anatomic-pathological report from systematic sextant biopsies showed Gleason score = 3 + 4



## Correlation between kinetic and static FCH PET/CT parameters

Results showed that K1 was moderately correlated with early SUVmean ( $r=0.57$ ;  $p<0.001$ ) and late SUVmean ( $r=0.43$ ;  $p<0.001$ ). No significant correlation was observed between K1 and retention index ( $r = -0.11$ ;  $p=0.396$ ) (Fig. 2).

## Comparisons between FCH PET/CT parameters and clinicopathological characteristics

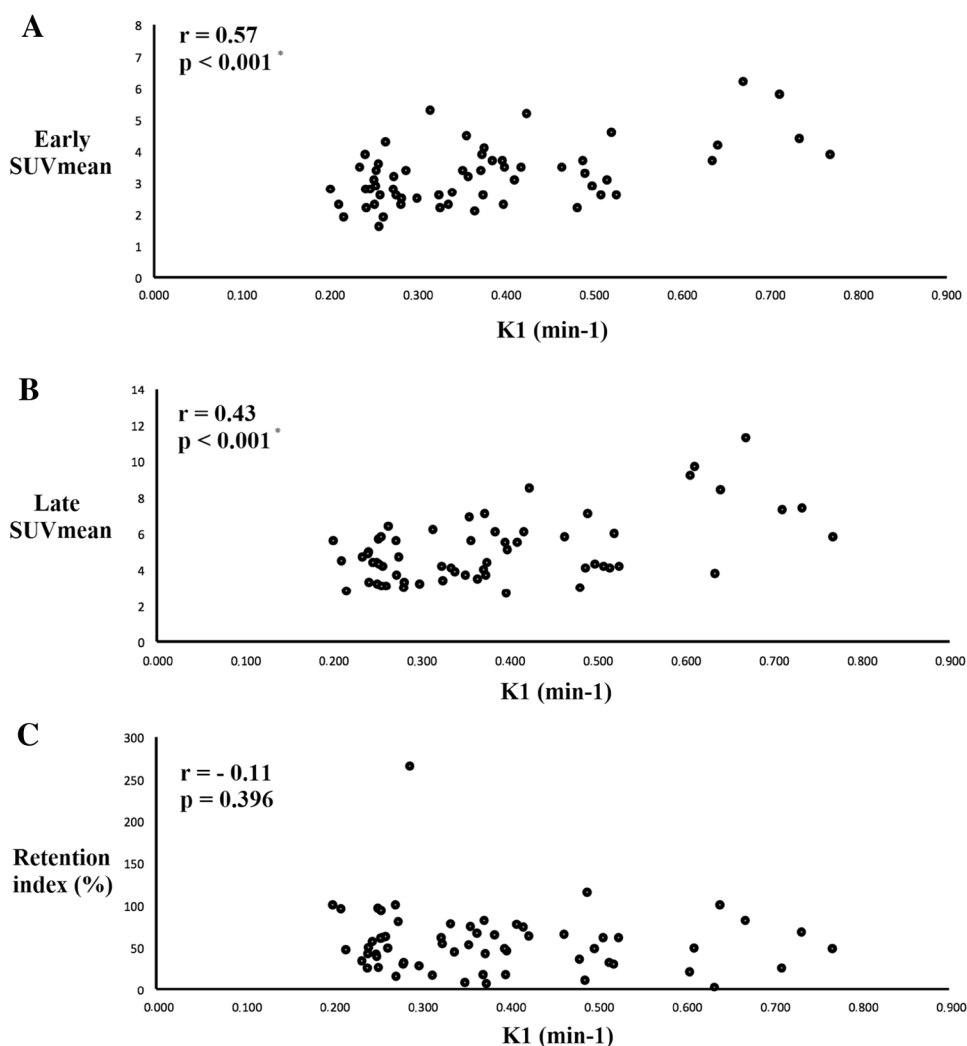
K1, early SUVmean, and late SUVmean were moderately correlated with PSA level (respectively,  $r=0.36$ ,  $p=0.004$ ;  $r=0.67$ ,  $p<0.001$ ;  $r=0.51$ ,  $p<0.001$ ) (Fig. 3). Concerning GS, the results of the Mann–Whitney U test showed that K1 was significantly higher for patients with  $GS \geq 4+3$  than for patients with  $GS < 4+3$ . No significant difference was observed for static parameters. Concerning the sub-group of patients with  $GS = 7$  (26 patients), only K1 parameter was

also significantly higher for patients with  $GS = 4+3$  than for patients with  $GS = 3+4$  (Table 1).

## Discussion

In this study, results show that FCH influx (K1) was the only FCH PET/CT parameter that is related to GS. To the best of our knowledge, only two studies with a lower number of participants compared kinetic FCH parameters and GS. Schaefferkoetter et al. demonstrated that FCH influx was significantly higher in tumors with GS of 4+3 than tumor with GS of 3+4 or 3+5 [24], which are consistent with the results of our study [24]. However, on the other hand, Choi et al. showed no difference between high and low GS [17]. Controversial results could be explained by a different kinetic modeling used between these studies (Schaefferkoetter et al. were using the one-tissue compartment model and Choi et al. were using the the two-tissue compartment

**Fig. 2** The Pearson's correlation analysis showing moderate but significant association between early SUVmean (a), late SUVmean (b) and K1. No significant association was observed between retention index and K1 (c)



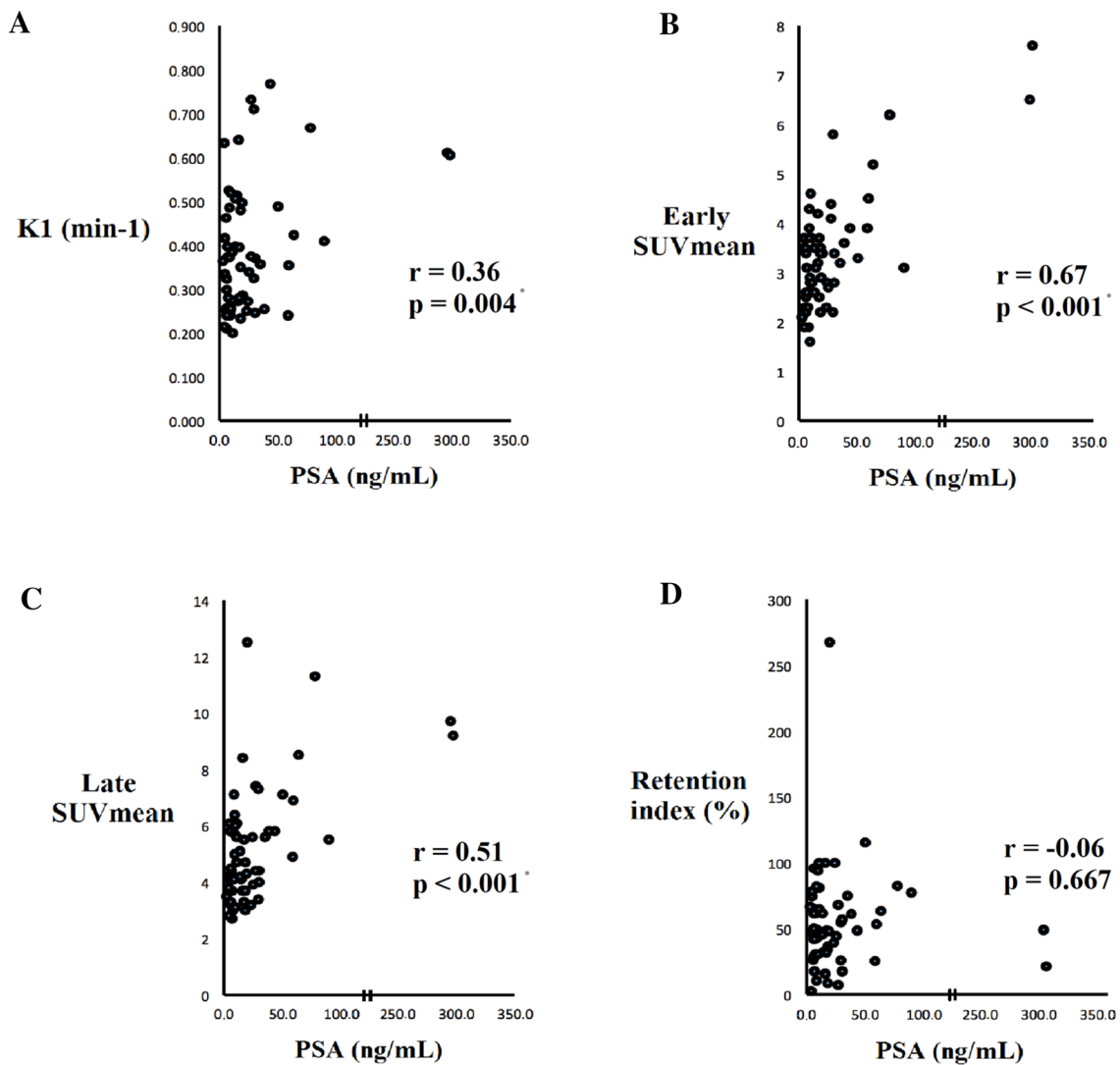


**Fig. 3** Pearson's correlation analysis showing moderate but significant association between K1 (a), early SUVmean (b) and late SUVmean (c) and PSA level. No significant association was observed between retention index and PSA level (d)

**Table 1** Comparison of FCH PET/CT parameters and Gleason scoring

	All of Gleason score			Gleason score = 7		
	≥ 4 + 3	< 4 + 3	<i>p</i>	4 + 3	3 + 4	<i>p</i>
K1 (min <sup>-1</sup> )	0.409	0.272	< 0.001*	0.438	0.281	0.027*
Early SUV mean	3.4	2.8	0.120	3.3	3.5	0.812
Late SUVmean	5.5	4.4	0.06	5.0	4.7	0.242
Retention index (%)	62	44	0.131	49	39	0.421

Statistical analysis was performed with the Mann–Whitney *U* test

\* *p* value < 0.05 = statistically significant

model). Furthermore, only 10 and 12 participants, respectively, were included.

Concerning static parameters and GS, results remain also controversial. In contrast to the results of our study, Schaefferkoetter et al. showed that 60-min SUV were

higher for GS of 4 + 3 than GS of 3 + 4 or 3 + 5 [24]. However, studies with a larger group of patients showed consistent results with our study. Indeed, Beheshti et al., De Perrot et al., and Choi et al. found no significant correlation between static parameters and Gleason scores [17,



27, 28]. The lack of significance could be explained by a reduced number of participants.

In the current study, we observed a significant but moderate correlation between K1 and early SUVmean. This result is consistent with the results from the study of Verwer et al. who recently reported showing poor correlation between K1 and SUV ( $r=0.30$ ) [26]. Furthermore, Takesh et al. showed also a poor correlation between K1 and SUVmean ( $r=0.28$ ) [20]. In the same way, Choi et al. did not show any significant correlation between K1 with other PET imaging parameters [17]. This poor correlation between kinetic and static parameters could explain the difference of correlation with GS for these two kinds of PET parameters. These results confirm that kinetic parameters may provide different metabolic information from static parameters.

Concerning PSA level at the time of FCH PET/CT examination, results showed that K1, early SUVmean and late SUVmean are correlated with PSA level. Many studies already showed correlations between static parameters and PSA level concerning FCH PET/CT for patients with recurrence of PC [17, 29–31]. That could explain why FCH PET/CT studies showed a low sensitivity to detect lesions in patients referred for recurrent PC with PSA level  $< 1$  ng/mL [29, 32].

Then, it is relevant to notice in our study that prostatic tumors showed a median retention index as 50%. These results are consistent with dual-phase FCH PET/CT studies [27, 33], showing higher retention for cancers than for benign lesions. However, our results indicate that K1 values were not significantly correlated with retention index. These results confirm that retention index and K1 represent two different molecular interactions. Indeed, Takesh et al. supposed that FCH uptake at later time points is linked to choline kinase activity whereas K1 is linked to perfusion [20]. In the current study, perfusion through K1 is correlated with GS, whereas choline kinase activity through the retention index is not. Further studies are needed to investigate the eventual correlation of K1 with angiogenesis and, under this suggestion, to assess if K1 could be a tool to predict the tumor aggression.

The current study presents limitations. First, an imaging-derived arterial input function was used for the kinetic modeling instead of a conventional plasma-derived input function. In traditional kinetic modeling, a plasma-derived input function is usually obtained from arterial sampling with a metabolite correction, which is relatively invasive and complex to perform in a routine clinical setting. However, Verwer et al. recently reported that the use of an imaging-derived plasma input function was feasible for a kinetic analysis [26]. Second, an easy homogenous time sampling (20 frames of 30 s) for dynamic PET data was preferred to be adapted for clinical assessment. This time sampling is not optimized for the imaging-derived plasma input function,

but kinetic parameters were compared in patients who performed the same FCH PET/CT protocol.

## Conclusions

The results of this study showed that FCH influx index K1 seems to be related to GS. Further analyses are required to confirm that K1 could distinguish well-differentiated from least-differentiated and could be a non-invasive tool to gain further information concerning tumor aggressiveness. FCH PET/CT is useful in detecting metastases in patients with biochemical recurrence, but it may play an important role also in initial tumor staging similar to and in conjunction with MRI-supported biopsy and potentially improve patient management with dose escalation for PC lesions with higher K1 using intensity-modulated radiotherapy.

## Compliance with ethical standards

**Conflict of interest** The authors declare that they have no conflicts of interest.

**Ethical approval** All procedures performed in studies involving human participants were in accordance with the ethical standards of the institutional and/or national research committee and with the 1964 Helsinki declaration and its later amendments or comparable ethical standards.

**Informed consent** Informed consent was obtained from all individual participants included in the study.

## References

1. Zhou CK, Check DP, Lortet-Tieulent J, Laversanne M, Jemal A, Ferlay J, et al. Prostate cancer incidence in 43 populations worldwide: An analysis of time trends overall and by age group. *Int J Cancer*. 2016;138(6):1388–400.
2. Cimitan M, Evangelista L, Hodolic M, Mariani G, Baseric T, Bodanza V, et al. Gleason score at diagnosis predicts the rate of detection of 18F-choline PET/CT performed when biochemical evidence indicates recurrence of prostate cancer: experience with 1,000 patients. *J Nucl Med Off Publ Soc Nucl Med*. 2015;56(2):209–15.
3. Oyen WJ, De Jong IJ. Molecular imaging of prostate cancer: tapping into the opportunities. *J Nucl Med Off Publ Soc Nucl Med*. 2015;56(2):169–70.
4. DeGrado TR, Baldwin SW, Wang S, Orr MD, Liao RP, Friedman HS, et al. Synthesis and evaluation of (18)F-labeled choline analogs as oncologic PET tracers. *J Nucl Med Off Publ Soc Nucl Med*. 2001;42(12):1805–14.
5. DeGrado TR, Reiman RE, Price DT, Wang S, Coleman RE. Pharmacokinetics and radiation dosimetry of 18F-fluorocholine. *J Nucl Med Off Publ Soc Nucl Med*. 2002;43(1):92–6.
6. Jadvar H. Prostate cancer: PET with 18F-FDG, 18F- or 11C-acetate, and 18F- or 11C-choline. *J Nucl Med Off Publ Soc Nucl Med*. 2011;52(1):81–9.
7. Cornford P, Bellmunt J, Bolla M, Briers E, De Santis M, Gross T, et al. EAU-ESTRO-SIOG guidelines on prostate cancer. Part II:

- treatment of relapsing, metastatic, and castration-resistant prostate cancer. *Eur Urol*. 2017;71(4):630–42.
8. Schwarzenbock S, Souvatzoglou M, Krause BJ. Choline PET and PET/CT in primary diagnosis and staging of prostate cancer. *Theranostics*. 2012;2(3):318–30.
  9. Mottet N, Bellmunt J, Bolla M, Briers E, Cumberbatch MG, De Santis M, et al. EAU-ESTRO-SIOG guidelines on prostate cancer. Part 1: screening, diagnosis, and local treatment with curative intent. *Eur Urol*. 2017;71(4):618–29.
  10. Rodrigues G, Warde P, Pickles T, Crook J, Brundage M, Souhami L, et al. Pre-treatment risk stratification of prostate cancer patients: a critical review. *Can Urol Assoc J J de l'Assoc des Urol du Can*. 2012;6(2):121–7.
  11. Boychak O, Vos L, Makis W, Buteau FA, Pervez N, Parliament M, et al. Role for (11)C-choline PET in active surveillance of prostate cancer. *Can Urol Assoc J J de l'Assoc des Urol du Can*. 2015;9(3–4):E98–E103.
  12. Beheshti M, Haim S, Zakavi R, Steinmair M, Waldenberger P, Kunit T, et al. Impact of 18F-choline PET/CT in prostate cancer patients with biochemical recurrence: influence of androgen deprivation therapy and correlation with PSA kinetics. *J Nucl Med Off Publ Soc Nucl Med*. 2013;54(6):833–40.
  13. Giovacchini G, Picchio M, Garcia-Parra R, Briganti A, Abdollah F, Gianolli L, et al. 11C-choline PET/CT predicts prostate cancer-specific survival in patients with biochemical failure during androgen-deprivation therapy. *J Nucl Med Off Publ Soc Nucl Med*. 2014;55(2):233–41.
  14. Morigi JJ, Stricker PD, van Leeuwen PJ, Tang R, Ho B, Nguyen Q, et al. Prospective comparison of 18F-fluoromethylcholine versus 68 Ga-PSMA PET/CT in prostate cancer patients who have rising PSA after curative treatment and are being considered for targeted therapy. *J Nucl Med Off Publ Soc Nucl Med*. 2015;56(8):1185–90.
  15. Beheshti M, Langsteger W. PET imaging of prostate cancer using radiolabeled choline. *PET Clinics*. 2009;4(2):173–84.
  16. Chondrogiannis S, Marzola MC, Grassetto G, Rampin L, Massaro A, Colletti PM, et al. Optimized protocol for (18)F-choline PET/CT in patients with biochemically relapsed prostate cancer: experiences on 250 consecutive cases. *Clin Nucl Med*. 2015;40(6):e308–12.
  17. Choi JY, Yang J, Noworolski SM, Behr S, Chang AJ, Simko JP, et al. 18F fluorocholine dynamic time-of-flight PET/MR imaging in patients with newly diagnosed intermediate- to high-risk prostate cancer: initial clinical-pathologic comparisons. *Radiology*. 2017;282(2):429–36.
  18. Mathieu C, Ferrer L, Carlier T, Colombie M, Rusu D, Kraeber-Bodere F, et al. Assessment of lymph nodes and prostate status using early dynamic curves with (18)F-choline PET/CT in prostate cancer. *Front Med*. 2015;2:67.
  19. Rosenkrantz AB, Koesters T, Vahle AK, Friedman K, Bartlett RM, Taneja SS, et al. Quantitative graphical analysis of simultaneous dynamic PET/MRI for assessment of prostate cancer. *Clin Nucl Med*. 2015;40(4):e236–e240.
  20. Takesh M. Kinetic modeling application to (18)F-fluoroethylcholine positron emission tomography in patients with primary and recurrent prostate cancer using two-tissue compartmental model. *World J Nucl Med*. 2013;12(3):101–10.
  21. Kristian A, Revheim ME, Qu H, Maelandsmo GM, Engebraten O, Seierstad T, et al. Dynamic (18)F-FDG-PET for monitoring treatment effect following anti-angiogenic therapy in triple-negative breast cancer xenografts. *Acta Oncol*. 2013;52(7):1566–72.
  22. Schierz JH, Opfermann T, Steenbeck J, Lopatta E, Settmacher U, Stallmach A, et al. Early dynamic 18F-FDG PET to detect hyperperfusion in hepatocellular carcinoma liver lesions. *J Nucl Med Off Publ Soc Nucl Med*. 2013;54(6):848–54.
  23. Strauss LG, Koczan D, Klippel S, Pan L, Willis S, Sachpekidis C, et al. Dynamic PET with (18)F-deoxyglucose (FDG) and quantitative assessment with a two-tissue compartment model reflect the activity of glucose transporters and hexokinases in patients with colorectal tumors. *Am J Nucl Med Mol Imaging*. 2013;3(5):417–24.
  24. Schaefferkoetter JD, Wang Z, Stephenson MC, Roy S, Conti M, Eriksson L, et al. Quantitative 18F-fluorocholine positron emission tomography for prostate cancer: correlation between kinetic parameters and Gleason scoring. *EJNMMI Res*. 2017;7(1):25.
  25. Daisne JF, Duprez T, Weynand B, Lonneux M, Hamoir M, Reyckler H, et al. Tumor volume in pharyngolaryngeal squamous cell carcinoma: comparison at CT, MR imaging, and FDG PET and validation with surgical specimen. *Radiology*. 2004;233(1):93–100.
  26. Verwer EE, Oprea-Lager DE, van den Eertwegh AJ, van Moorseelaar RJ, Windhorst AD, Schwarte LA, et al. Quantification of 18F-fluorocholine kinetics in patients with prostate cancer. *J Nucl Med Off Publ Soc Nucl Med*. 2015;56(3):365–71.
  27. Beheshti M, Imamovic L, Broinger G, Vali R, Waldenberger P, Stoiber F, et al. 18F choline PET/CT in the preoperative staging of prostate cancer in patients with intermediate or high risk of extracapsular disease: a prospective study of 130 patients. *Radiology*. 2010;254(3):925–33.
  28. de Perrot T, Rager O, Scheffler M, Lord M, Pusztaszeri M, Iselein C, et al. Potential of hybrid (1)(8)F-fluorocholine PET/MRI for prostate cancer imaging. *Eur J Nucl Med Mol Imaging*. 2014;41:1744–55.
  29. Evangelista L, Briganti A, Fanti S, Joniau S, Reske S, Schiavina R, et al. New clinical indications for (18)F/(11)C-choline, new tracers for positron emission tomography and a promising hybrid device for prostate cancer staging: a systematic review of the literature. *Eur Urol*. 2016;70(1):161–75.
  30. Krause BJ, Souvatzoglou M, Tuncel M, Herrmann K, Buck AK, Praus C, et al. The detection rate of [11C]choline-PET/CT depends on the serum PSA-value in patients with biochemical recurrence of prostate cancer. *Eur J Nucl Med Mol Imaging*. 2008;35(1):18–23.
  31. Castellucci P, Fuccio C, Nanni C, Santi I, Rizzello A, Lodi F, et al. Influence of trigger PSA and PSA kinetics on 11C-choline PET/CT detection rate in patients with biochemical relapse after radical prostatectomy. *J Nucl Med Off Publ Soc Nucl Med*. 2009;50(9):1394–400.
  32. Mapelli P, Incerti E, Ceci F, Castellucci P, Fanti S, Picchio M. 11C- or 18F-choline PET/CT for imaging evaluation of biochemical recurrence of prostate cancer. *J Nucl Med Off Publ Soc Nucl Med*. 2016;57(Suppl 3):43S–48S.
  33. Kwee SA, Wei H, Sesterhenn I, Yun D, Coel MN. Localization of primary prostate cancer with dual-phase 18F-fluorocholine PET. *J Nucl Med Off Publ Soc Nucl Med*. 2006;47(2):262–9.